Connecting the Popularity Adjusted Block Model to the Generalized Random Dot Product Graph for Clustering and Parameter Estimation

John Koo, Minh Tang, Michael Trosset

Abstract

In this paper, we connect two random graph models, the Popularity Adjusted Block Model (PABM) and the Generalized Random Dot Product Graph (GRDPG) and use properties established in this connection to aid in community detection and parameter estimation. In particular, we note that the PABM can be represented as latent positions such that points within the same community lie on a subspace, and the subspaces that represent each community are orthogonal to one another. Using this property as well as the asymptotic properties of Adjacency Spectral Embedding (ASE) of the GRDPG, we are able to establish theoretical asymptotic results of our community detection and parameter estimation methods for the PABM.

1 Introduction

Statistical analysis on graphs or networks often involves the partitioning of a graph into disconnected subgraphs or clusters. This is often motivated by the belief that there exist underlying and unobserved communities to which each vertex of the graph belongs, and edges between pairs of vertices are determined by drawing from a probability distribution based on the community relationships between each pair. The goal of this analysis then is population community detection, or the recovery of the true underlying community labels for each vertex, up to permutation (with some additional parameter estimation being of possible interest), assuming some random graph model. One such model is the Stochastic Block Model (SBM), first proposed by Lorrain and White [11], which assumes that the edge probability from one vertex to another follows a Beronulli distribution with fixed probabilities for each pair of community labels. Other random graph models have been proposed and studied, such as the Degree-Corrected Block Model (DCBM), introduced by Karrer and Newman [9] and the Mixed Membership Stochastic Block Model (MMSBM), introduced by Airoldi, Blei, Fienberg, and Xing [2]. The Popularity Adjusted Block Model (PABM) was then introduced by Sengupta and Chen [16] as a generalization of the SBM to address the heterogeneity of edge probabilities within and between communities while still maintaining distinct community structure.

The underlying similarity among the SBM, PABM, and other such models is that they involve

a symmetric edge probability matrix $P \in [0,1]^{n \times n}$ where n is the number of vertices in the graph. An undirected and unweighted graph is then drawn from this edge probability matrix such that the existence of an edge between each pair of vertices i and j is given by Bernoulli(P_{ij}). For example, for the SBM with two communities for which the within-community edge probability is ξ and the between-community edge probability is η, the entries of P consist of ξ and η.

The Random Dot Product Graph (RDPG) model proposed by Young and Scheinerman [19] is another graph model with Bernoulli edge probabilities. Under this model, each vertex of the graph can be represented by a point in a latent Euclidean space such that the edge probability between any pair of vertices is given by their corresponding dot product in the latent space, i.e., given a latent positions $x_1, ..., x_n \in \mathbb{R}^d$, the edge probability matrix is $P = XX^\top$ where $X = \begin{bmatrix} x_1 & \cdots & x_n \end{bmatrix}^\top$. The SBM is equivalent to a special case of the RDPG model in which all vertices of a given community share the same position in the latent space [12]. It has also been shown that similar random graph models, including both the MMSBM and DCBM, can be represented in this way [15] [12]. An analogous property exists for the PABM but not for the RDPG model but under the *Generalized* Random Dot Product Graph (GRDPG) model. This relationship will be explored in this paper and exploited to construct algorithms for community detection and parameter estimation for the PABM.

In this paper, we will only consider undirected graphs, that is the edge weight from vertex i to vertex j is equal to the edge weight in the opposite direction, from vertex j to vertex i. Furthermore, we will only consider unweighted graphs with binary $(0,1)$ edge weights We will also assume that graphs are hollow, i.e., there are no edges from a vertex to itself. All such graphs can be represented by a symmetric adjacency matrix $A \in \{0,1\}^{n \times n}$ for which $A_{ij} = 1$ if there exists an edge between vertices i and j and 0 otherwise, and A is an element-wise independent Bernoulli draw from a symmetric edge probability matrix $P \in [0,1]^{n \times n}$.

2 Connecting the Popularity Adjusted Block Model to the Generalized Random Dot Product Graph

2.1 The popularity adjusted block model (PABM) and the generalized random dot product graph

Definition 1 (Popularity Adjusted Block Model) [16]. Let $P \in [0,1]^{n \times n}$ be a symmetric edge probability matrix for a set of n vertices, V. Each vertex has a community label $1, ..., K$, and the rows and columns of P are arranged by community label such that $n_k \times n_l$ block $P^{(kl)}$ describes the edge probabilities between vertices in communities k and l $(P^{(lk)} = (P^{(kl)})^\top)$. Let graph $G = (V, E)$ be an undirected, unweighted graph such that its corresponding adjacency matrix $A \in \{0,1\}^{n \times n}$ is a realization of Bernoulli(P), i.e., $A_{ij} \overset{\text{indep}}{\sim}$ Bernoulli(P_{ij}) for $i > j$ $(A_{ij} = A_{ji}$ and $A_{ii} = 0)$.

If each block $P^{(kl)}$ can be written as the outer product of two vectors:

$$P^{(kl)} = \lambda^{(kl)}(\lambda^{(lk)})^\top \tag{1}$$

for a set of K^2 fixed vectors $\{\lambda^{(st)}\}_{s,t=1}^K$ where each $\lambda^{(st)}$ is a column vector of dimension n_s, then graph G and its corresponding adjacency matrix A is a realization of a popularity adjusted block model with parameters $\{\lambda^{(st)}\}_{s,t=1}^K$.

We will use the notation $A \sim PABM(\{\lambda^{(kl)}\}_K)$ to denote a random adjacency matrix A drawn from a PABM with parameters $\lambda^{(kl)}$ consisting of K underlying communities.

Definition 2 (Generalized Random Dot Product Graph) [14]. Let $P \in [0,1]^{n \times n}$ be a symmetric edge probability matrix for a set of n vertices, V. If $\exists X \in \mathbb{R}^{n \times d}$ such that

$$P = X I_{pq} X^\top \tag{2}$$

for some $d, p, q \in \mathbb{N}$ and $p + q = d$, then graph $G = (V, E)$ with adjacency matrix A such that $A_{ij} \overset{\text{indep}}{\sim} \text{Bernoulli}(P_{ij})$ for $i > j$ ($A_{ij} = A_{ji}$ and $A_{ii} = 0$) is a draw from the generalized random dot product graph model with latent positions X and signature (p, q). More precisely, if vertices i and j have latent positions x_i and x_j respectively, then the edge probability between the two is $P_{ij} = x_i^\top I_{pq} x_j$, and X contains the latent positions as rows $x_i^\top$.

We will use the notation $A \sim GRDPG_{p,q}(X)$ to denote a random adjacency matrix A drawn from latent positions X and signature (p, q).

Definition 3. The indefinite orthogonal group with signature (p, q) is the set $\{Q \in \mathbb{R}^{d \times d} : Q I_{pq} Q^\top = I_{pq}\}$, denoted as $\mathbb{O}(p, q)$ [14].

Remark. Like the RDPG, the latent positions of a GRDPG are not unique [14]. More specifically, if $P_{ij} = x_i^\top I_{pq} x_j$, then we also have for any $Q \in \mathbb{O}(p, q)$, $(Qx_i)^\top I_{pq}(Qx_j) = x_i^\top(Q^\top I_{pq} Q)x_j = x_i^\top I_{pq} x_j = P_{ij}$. Unlike in the RDPG case, transforming the latent positions via multiplication by $Q \in \mathbb{O}(p, q)$ does not necessarily maintain interpoint angles or distances.

2.2 Connecting the PABM to the GRDPG

Theorem 1 (Connecting the PABM to the GRDPG for $K = 2$). Let

$$X = \begin{bmatrix} \lambda^{(11)} & \lambda^{(12)} & 0 & 0 \\ 0 & 0 & \lambda^{(21)} & \lambda^{(22)} \end{bmatrix}$$

$$U = \begin{bmatrix} 1 & 0 & 0 & 0 \\ 0 & 0 & 1/\sqrt{2} & 1/\sqrt{2} \\ 0 & 0 & 1/\sqrt{2} & -1/\sqrt{2} \\ 0 & 1 & 0 & 0 \end{bmatrix}$$

as in Definition 1. Then $A \sim GRDPG_{3,1}(XU)$ and $A \sim PABM(\{(\lambda^{(kl)}\}_2)$ are equivalent.

Proof. This is given by straightforward matrix multiplication. It suffices to show that

$$XUI_{3,1}U^\top X^\top = \begin{bmatrix} \lambda^{(11)}(\lambda^{(11)})^\top & \lambda^{(12)}(\lambda^{(21)})^\top \\ \lambda^{(21)}(\lambda^{(12)})^\top & \lambda^{(22)}(\lambda^{(22)})^\top \end{bmatrix}$$

Remark. While we can just perform the matrix multiplication to show the equivalence, it is more illustrative to look at a few intermediate steps. Note that the product of the three inner matrices results in a permutation matrix with fixed points at positions 1 and 4 and a cycle of order 2 swappoing positions 2 and 3:

$$UI_{3,1}U^\top = \begin{bmatrix} 1 & 0 & 0 & 0 \\ 0 & 0 & 1 & 0 \\ 0 & 1 & 0 & 0 \\ 0 & 0 & 0 & 1 \end{bmatrix} = \Pi$$

Since U is orthonormal and $I_{3,1}$ is diagonal, $\Pi = UI_{3,1}U^\top$ is a spectral decomposition of this permutation matrix. Note that the two fixed points result in eigenvalues of $+1$ with corresponding eigenvectors e_i where $i = 1, 4$ corresponding to the locations of the fixed points, and the cycle of order two results in two eigenvalues ± 1 with corresponding eigenvectors $(e_i \pm e_j)/\sqrt{2}$ where $i = 2, j = 3$, pair that is swapped.

Theorem 2 (Generalization to $K > 2$). There exists a block diagonal matrix $X \in \mathbb{R}^{n \times K^2}$ defined by PABM parameters $\{\lambda^{(kl)}\}_K$ and $U \in \mathbb{R}^{K^2 \times K^2}$ that is fixed for each K such that $A \sim GRDPG_{K(K+1)/2, K(K-1)/2}(XU)$ and $A \sim PABM(\{(\lambda^{(kl)}\})_K)$ are equivalent.

Proof. Let

$$\Lambda^{(k)} = \begin{bmatrix} \lambda^{(k,1)} & \cdots & \lambda^{(k,K)} \end{bmatrix} \in \mathbb{R}^{n_k \times K}$$

$$X = \text{blockdiag}(\Lambda^{(1)}, ..., \Lambda^{(K)}) \in \mathbb{R}^{n \times K^2} \tag{3}$$

$$L^{(k)} = \text{blockdiag}(\lambda^{(1k)}, ..., \lambda^{(Kk)}) \in \mathbb{R}^{n \times K}$$

$$Y = \begin{bmatrix} L^{(1)} & \cdots & L^{(K)} \end{bmatrix} \in \mathbb{R}^{n \times K^2}$$

Then $P = XY^\top$.

Similar to the $K = 2$ case, we have $Y = X\Pi$ for a permutation matrix Π, resulting in $P = X\Pi X^\top$.

The permutation described by Π has K fixed points, which correspond to K eigenvalues equal to 1 with corresponding eigenvectors e_k where $k = r(K + 1) + 1$ for $r = 0, ..., K - 1$. It also has $\binom{K}{2} = K(K-1)/2$ cycles of order 2. Each cycle corresponds to a pair of eigenvalues $+1$ and -1 and a pair of eigenvectors $(e_s + e_t)/\sqrt{2}$ and $(e_s - e_t)/\sqrt{2}$.

Then Π has $K(K+1)/2$ eigenvalues equal to 1 and $K(K-1)/2$ eigenvalues equal to -1. Π has the decomposed form

$$\Pi = U I_{K(K+1)/2, K(K-1)/2} U^\top \tag{4}$$

The edge probability matrix then can be written as:

$$P = X U I_{p,q}(XU)^\top \tag{5}$$

$$p = K(K+1)/2 \tag{6}$$

$$q = K(K-1)/2 \tag{7}$$

and we can describe the PABM with K communities as a GRDPG with latent positions XU with signature $\big(K(K+1)/2, K(K-1)/2\big)$.

Example $(K = 3)$. Using the same notation as before:

$$X = \begin{bmatrix} \lambda^{(11)} & \lambda^{(12)} & \lambda^{(13)} & 0 & 0 & 0 & 0 & 0 & 0 \\ 0 & 0 & 0 & \lambda^{(21)} & \lambda^{(22)} & \lambda^{(23)} & 0 & 0 & 0 \\ 0 & 0 & 0 & 0 & 0 & 0 & \lambda^{(31)} & \lambda^{(32)} & \lambda^{(33)} \end{bmatrix}$$

$$Y = \begin{bmatrix} \lambda^{(11)} & 0 & 0 & \lambda^{(12)} & 0 & 0 & \lambda^{(13)} & 0 & 0 \\ 0 & \lambda^{(21)} & 0 & 0 & \lambda^{(22)} & 0 & 0 & \lambda^{(23)} & 0 \\ 0 & 0 & \lambda^{(31)} & 0 & 0 & \lambda^{(32)} & 0 & 0 & \lambda^{(33)} \end{bmatrix}$$

Then $P = XY^\top$ and $Y = X\Pi$ where Π is a permutation matrix consisting of 3 fixed points and 3 cycles of order 2:

$$\Pi = \begin{bmatrix} 1 & 0 & 0 & 0 & 0 & 0 & 0 & 0 & 0 \\ 0 & 0 & 0 & 1 & 0 & 0 & 0 & 0 & 0 \\ 0 & 0 & 0 & 0 & 0 & 0 & 1 & 0 & 0 \\ 0 & 1 & 0 & 0 & 0 & 0 & 0 & 0 & 0 \\ 0 & 0 & 0 & 0 & 1 & 0 & 0 & 0 & 0 \\ 0 & 0 & 0 & 0 & 0 & 0 & 0 & 1 & 0 \\ 0 & 0 & 1 & 0 & 0 & 0 & 0 & 0 & 0 \\ 0 & 0 & 0 & 0 & 0 & 1 & 0 & 0 & 0 \\ 0 & 0 & 0 & 0 & 0 & 0 & 0 & 0 & 1 \end{bmatrix}$$

- Positions 1, 5, 9 are fixed.
- The cycles of order 2 are $(2, 4)$, $(3, 7)$, and $(6, 8)$.

Therefore, we can decompose $\Pi = U I_{6,3} U^\top$ where the first three columns of U consist of e_1, e_5, and e_9 corresponding to the fixed positions 1, 5, and 9, the next three columns consist of eigenvectors $(e_k + e_l)/\sqrt{2}$, and the last three columns consist of eigenvectors $(e_k - e_l)/\sqrt{2}$, where pairs (k, l) correspond to the cycles of order 2 described above.

The latent positions are the rows of

$$
XU = \begin{bmatrix}
\lambda^{(11)} & 0 & 0 & \lambda^{(12)}/\sqrt{2} & \lambda^{(13)}/\sqrt{2} & 0 & \lambda^{(12)}/\sqrt{2} & \lambda^{(13)}/\sqrt{2} & 0 \\
0 & \lambda^{(22)} & 0 & \lambda^{(21)}/\sqrt{2} & 0 & \lambda^{(23)}/\sqrt{2} & -\lambda^{(21)}/\sqrt{2} & 0 & \lambda^{(23)}/\sqrt{2} \\
0 & 0 & \lambda^{(33)} & 0 & \lambda^{(31)}/\sqrt{2} & \lambda^{(32)}/\sqrt{2} & 0 & -\lambda^{(31)}/\sqrt{2} & -\lambda^{(32)}/\sqrt{2}
\end{bmatrix}
$$

3 Methods

Two inference objectives arise from the PABM:

1. Community membership identification (up to permutation).
2. Parameter estimation (estimating $\lambda^{(kl)}$'s).

In our methods, we assume that K, the number of communities, is known beforehand and does not require estimation.

3.1 Related work

Sengupta and Chen [16], who first proposed the PABM, used modularity maximization for clustering and parameter estimation. They were able to show that as the sample size increases, the proportion of misclassified community labels (up to permutation) goes to 0. However, because modularity maximization is NP-hard, the authors of this paper used an approximation based on the Extreme Points algorithm [10].

Noroozi, Rimal, and Pensky [13] proposed using sparse subspace clustering to identify the community memberships given either an edge probability matrix P or an adjacency matrix A. In the case that P is known, the community memberships can be identified exactly (up to permutation). This is supported by our Theorem 2, which shows that the ASE of edge probability matrix P consists of K K-dimensional subspaces lying in $\mathbb{R}^{K^2}$. A similar procedure can be applied if P is unknown and we have an observation A, but the theoretical guarantees of this method applied to the PABM are unknown.

3.2 Community detection

3.2.1 Using edge probability matrix P

We previously stated one possible set of latent positions that result in the edge probability matrix of a PABM, $P = (XU)I_{pq}(XU)^\top$. If we have (or can estimate) XU directly, then both the community detection and parameter identification problem are trivial since U is orthonormal and fixed for each value of K. However, direct identification or estimation of XU is not possible [14].

If we decompose $P = Z I_{pq} Z^\top$, then $\exists Q \in \mathbb{O}(p, q)$ such that $XU = ZQ$. Even if we start with the exact edge probability matrix, we cannot recover the "original" latent positions XU. Note that unlike in the case of the RDPG, Q is not an orthogonal matrix. If z_i's are the rows of XU, then $||z_i - z_j||^2 \neq ||Qz_i - Qz_j||^2$, and $\langle z_i, z_j \rangle \neq \langle Qz_i, Qz_j \rangle$. This prevents us from using the properties of XU directly. In particular, if $Q \in \mathbb{O}(n)$, then we could use the fact that $\langle z_i, z_j \rangle = \langle Qz_i, Qz_j \rangle = 0$ if vertices i and j are in different communities.

We can note from the explicit form of XU that it represents points in $\mathbb{R}^{K^2}$ such that points within each community lie on K-dimensional subspaces. Furthermore, the subspaces are orthogonal to each other. Multiplication by $Q \in \mathbb{O}(p, q)$ removes the orthogonality property but retains the property that each community is represented by a K-dimensional subspace. Using this property, previous work proposes the use of subspace clustering [13] [17].

Lemma 1. Let $P = VDV^\top$ be the spectral decomposition of the edge probability matrix for a PABM. Then $VV^\top = X(X^\top X)^{-1} X^\top$ where X is defined as in equation (3).

Proof. By Theorem 2, $P = XU I_{p,q} U^\top X^\top$, where X is defined as in equation (3) and p and q are defined as in equations (6) and (7). Alternatively, the spectral decomposition can be written as $P = VDV^\top = V|D|^{1/2} I_{p,q}|D|^{1/2} V^\top$ for the same (p, q) and $|\cdot|^{1/2}$ is applied entry-wise. Thus for some $Q \in \mathbb{O}(p, q)$,

$$XUQ = V|D|^{1/2}$$

Therefore, using the fact that $UU^\top = I$ and $V^\top V = I$,

$$(V|D|^{1/2})((V|D|^{1/2})^\top(V|D|^{1/2}))^{-1}(V|D|^{1/2})^\top = (XUQ)((XUQ)^\top(XUQ))^{-1}(XUQ)^\top$$

The righthand side becomes

$$\begin{aligned}(XUQ)((XUQ)^\top(XUQ))^{-1}(XUQ)^\top &= XUQQ^{-1}U^\top(X^\top X)^{-1}U(Q^\top)^{-1}Q^\top U^\top X^\top \\ &= XUU^\top(X^\top X)^{-1}UU^\top X^\top \\ &= X(X^\top X)^{-1}X^\top\end{aligned}$$

The lefthand side becomes:

$$\begin{aligned}(V|D|^{1/2})((V|D|^{1/2})^\top(V|D|^{1/2}))^{-1}(V|D|^{1/2})^\top &= V|D|^{1/2}|D|^{-1/2}(V^\top V)^{-1}|D|^{-1/2}|D|^{1/2}V^\top \\ &= VV^\top\end{aligned}$$

Theorem 3. Let $P = VDV^\top$ be the spectral decomposition of the edge probability matrix. Let $B = VV^\top$. Then $B_{ij} = 0$ if vertices i and j are of different communities.

Proof. By Lemma 1, $VV^\top = X(X^\top X)^{-1}X^\top$ where X is defined as in Theorem 2. Since X is block diagonal with each block corresponding to one community, $X(X^\top X)^{-1}X^\top$ is also a block diagonal matrix with each block corresponding to a community and zeros elsewhere. Therefore, if vertices i and j belong to different communities, then the ij^{th} element of $X(X^\top X)^{-1}X^\top = VV^\top = B$ is 0.

Algorithm 1: PABM clustering on the edge probability matrix.

Data: Edge probability matrix P, number of communities K
Result: Community labels $1, ..., K$

1 Compute the spectral decomposition $P = VDV^\top$.
2 Compute the inner product matrix $B = |VV^\top|$, applying $|\cdot|$ entry-wise.
3 Construct graph G using B as edge similarities.
4 Identify the connected components of G and map each to community labels $1, ..., K$.

3.2.2 Using adjacency matrix A

The adjacency embedding of A approaches latent positions that form P as the number of vertices n increases. More precisely, let $\{\lambda^{(kl)}\}_K \sim \mathcal{F}_K$ for some joint distribution consisting of K underlying communities $\mathcal{F}_K$. Then the latent positions $XU \sim \mathcal{G}_K$ for some related joint distribution with K underlying communities $\mathcal{G}_K$. Denote Z_n as a sample of size n from $\mathcal{G}_K$ and adjacency matrix A_n as one draw from edge probability matrix $P_n = Z_n I_{pq} Z_n^\top$. Let $\hat{Z}_n$ be the adjacency embedding of A_n with rows $(\hat{z}_i^{(n)})^\top$. Then by Rubin-Delanchy et al. [14],

$$\max_{i \in \{1,...,n\}} ||Q_n \hat{z}_i^{(n)} - z_i^{(n)}|| = O_P\left(\frac{(\log n)^c}{n^{1/2}}\right) \tag{8}$$

for some $c > 0$ and sequence of $Q_n \in \mathbb{O}(p, q)$. In addition, Rubin-Delanchy et al. produce a central limit theorem result.

Theorem 4. Let $\hat{V}^{(n)} \in \mathbb{R}^{n \times K^2}$ be the matrix of K^2 eigenvectors of A_n corresponding to the $K(K+1)/2$ most positive eigenvalues and $K(K-1)/2$ most negative eigenvalues with rows $(\hat{v}_i^{(n)})^\top$. Let (i,j) correspond to pairs belonging to different communities. Then for some $c > 0$,

$$\max_{i,j} ||(\hat{v}_i^{(n)})^\top \hat{v}_j^{(n)}|| = O_P\left(\frac{(\log n)^c}{n\sqrt{\rho_n}}\right) \tag{9}$$

where $\lim_{n \to 0} \rho_n = 0$ is a sparsity parameter introduced by Sengupta and Chen [16]. More precisely, $\rho_n = o(\log n/\sqrt{n})$ [14].

This leads to the following algorithm:

Algorithm 2: PABM clustering on the adjacency matrix.

Data: Adjacency matrix A, number of communities K

Result: Community assignments $1, ..., K$

1 Compute the eigenvectors of A that correspond to the $K(K+1)/2$ most positive eigenvalues and $K(K-1)/2$ most negative eigenvalues. Construct V using these eigenvectors as its columns.

2 Compute $B = |VV^\top|$, applying $|\cdot|$ entry-wise.

3 Construct graph G using B as its similarity matrix.

4 Partition G into K disconnected components (e.g., using edge thresholding or spectral clustering).

5 Map each partition to the community labels $1, ..., K$.

Theorem 4 implies that as $n \to \infty$, the number (not just proportion) of misclassified vertices, up to permutation, outputted by algorithm 2 goes to 0.

3.3 Parameter estimation

For any P edge probability matrix for the PABM such that the rows and columns are organized by community, the kl^th block is an outer product of two vectors, i.e., $P^{(kl)} = \lambda^{(kl)}(\lambda^{(lk)})^\top$. Therefore, given $P^{(kl)}$, λ and $\lambda^{(lk)}$ are solvable exactly (up to multiplication by -1) using singular value decomposition. More specifically, let $P = \sigma^2 uv^\top$ be the singular value decomposition of P. $u \in \mathbb{R}^{n_k}$ and $v \in \mathbb{R}^{n_l}$ are vectors and $\sigma^2 > 0$ is a scalar. Then $\lambda^{(kl)} = \pm\sigma u$ and $\lambda^{(lk)} = \pm\sigma v$.

Algorithm 3: PABM parameter estimation using the edge probability matrix.

Data: Edge probability matrix P, community assignments $1, ..., K$.

Result: PABM parameters $\{\lambda^{(kl)}\}_K$

1 Arrange the rows and columns of P by community such that each $P^{(kl)}$ block consists of edge probabilities between communities k and l.

2 **for** $k, l = 1, ..., K$, $k \geq l$ **do**

3 $\quad$ Compute $P^{(kl)} = (\sigma^{(kl)})^2 u^{(kl)}(v^{(kl)})^\top$, the SVD of the kl^{th} block.

4 $\quad$ Assign $\lambda^{(kl)} \leftarrow \pm\sigma^{(kl)}u^{(kl)}$ and $\lambda^{(lk)} \leftarrow \pm\sigma^{(kl)}v^{(kl)}$.

5 **end**

Given the adjacency matrix A instead of edge probability matrix P, we can simply use plug-in

estimators:

Algorithm 4: PABM parameter estimation using the adjacency matrix.

Data: Adjacency matrix A, community assignments $1, ..., K$

Result: PABM parameter estimates $\{\hat{\lambda}^{(kl)}\}_K$.

1 Arrange the rows and columns of A by community such that each $A^{(kl)}$ block consists of estimated edge probabilities between communities k and l.

2 for $k, l = 1, ..., K$, $k \leq l$ **do**

3   Compute $A^{(kl)} = U\Sigma V^\top$, the SVD of the kl^{th} block.

4   Assign $u^{(kl)}$ and $v^{(kl)}$ as the first columns of U and V. Assign $(\sigma^{(kl)})^2 \leftarrow \Sigma_{11}$.

5   Assign $\hat{\lambda}^{(kl)} \leftarrow \pm \sigma^{(kl)} u^{(kl)}$ and $\hat{\lambda}^{(lk)} \leftarrow \pm \sigma^{(kl)} v^{(kl)}$.

6 end

Theorem 5. Under regularity and sparsity assumptions, and under the further assumption that K is fixed and community labels are known,

$$\max_{k,l \in \{1,...,K\}} ||\hat{\lambda}^{(kl)} - \lambda^{(kl)}|| = O_P\left(\frac{(\log n_k)^c}{\sqrt{n_k}} \right) \tag{10}$$

Proof. Let P and A be organized by community such that the elements of blocks $P^{(kl)}$ and $A^{(kl)}$ correspond to the edges between communities k and l.

Case $k = l$. $P^{(kk)}$ and $A^{(kk)}$ represent within-community edge probabilities and edges for community k.

By definition, $P^{(kk)} = \lambda^{(kk)}(\lambda^{(kk)})^\top$. This implies that the signular value decomposition $P^{(kk)} = \sigma_{kk}^2 u^{(kk)}(u^{(kk)})^\top$ has one singular value and one pair of singular vectors ($P^{(kk)}$ is symmetric, so the left and right singular vectors are identical). Then $\lambda^{(kk)} = \sigma_{kk} u^{(kk)}$.

Let $\hat{U}^{(kk)}\hat{\Sigma}^{(kk)}(\hat{U}^{(kk)})^\top$ be the singular value decomposition of $A^{(kk)}$, and let $\hat{\sigma}_{kk}^2 \hat{u}^{(kk)}(\hat{u}^{(kk)})^\top$ be its one-dimensional approximation. Define $\hat{\lambda}^{(kk)} = \hat{\sigma}_{kk} \hat{u}^{(kk)}$. Then $\hat{\lambda}^{(kk)}$ is the adjacency spectral embedding approximation of $\lambda^{(kk)}$.

Then by Theorem 5 from Rubin-Delanchy et al. [14], the adjacency spectral embedding $\hat{\lambda}^{(kk)}$ approximates $\lambda^{(kk)}$ at rate $\frac{(\log n_k)^c}{\sqrt{n_k}}$.

Case $k \neq l$. $P^{(kl)}$ and $A^{(kl)}$ represent edge probabilities and edges between communities k and l. Note that $P^{(kl)} = (P^{(lk)})^\top$.

By definition, $P^{(kl)} = \lambda^{(kl)}(\lambda^{(lk)})^\top$. As in the $k = l$ case, we note that the singular value decomposition $P^{(kl)} = \sigma_{kl}^2 u^{(kl)}(v^{(kl)})^\top$ is one-dimensional and $\lambda^{(kl)} = \sigma_{kl} u^{(kl)}$. (We can also note that the SVD of $P^{(lk)} = \sigma_{kl}^2 v^{(kl)}(u^{(kl)})^\top$, i.e., $\sigma_{kl} = \sigma_{lk}$, $u^{(kl)} = v^{(lk)}$, and $v^{(kl)} = u^{(lk)}$.) Now consider the Hermitian dilation

$$M^{(kl)} = 2 \begin{bmatrix} 0 & P^{(kl)} \\ P^{(lk)} & 0 \end{bmatrix}$$

which is a symmetric $(n_k + n_l) \times (n_k + n_l)$ matrix. It can be shown that the eigendecomposition of $M^{(kl)}$ is

10

$$M^{(kl)} = \begin{bmatrix} u^{(kl)} & -u^{(kl)} \\ v^{(kl)} & v^{(kl)} \end{bmatrix} \times \begin{bmatrix} \sigma_{kl}^2 & 0 \\ 0 & -\sigma_{kl}^2 \end{bmatrix} \times \begin{bmatrix} u^{(kl)} & -u^{(kl)} \\ v^{(kl)} & v^{(kl)} \end{bmatrix}^\top$$

Thus treating $M^{(kl)}$ as the edge probability matrix of a GRDPG, we have latent positions in $\mathbb{R}^2$ given by

$$\begin{bmatrix} \sigma_{kl} u^{(kl)} & \sigma_{kl} u^{(kl)} \\ \sigma_{kl} v^{(kl)} & -\sigma_{kl} v^{(kl)} \end{bmatrix} = \begin{bmatrix} \lambda^{(kl)} & \lambda^{(kl)} \\ \lambda^{(lk)} & -\lambda^{(lk)} \end{bmatrix}$$

Now consider

$$\hat{M}^{(kl)} = \begin{bmatrix} 0 & A^{(kl)} \\ A^{(lk)} & 0 \end{bmatrix}$$

Then $\hat{M}^{(kl)} = M^{(kl)} + E'$ where

$$E' = \begin{bmatrix} 0 & E \\ E^\top & 0 \end{bmatrix}$$

and E is the $n_k \times n_l$ matrix of independent noise (to generate the Bernoulli entries in $A^{(kl)}$. Then $\hat{M}^{(kl)}$ is an adjacency matrix drawn from $M^{(kl)}$, so its adjacency spectral embedding, given by

$$\begin{bmatrix} \hat{\lambda}^{(kl)} & \hat{\lambda}^{(kl)} \\ \hat{\lambda}^{(lk)} & -\hat{\lambda}^{(lk)} \end{bmatrix}$$

where each $\hat{\lambda}^{(kl)}$ is defined as in Algorithm 4, approximates the latent positions of $M^{(kl)}$ up to indefinite orthogonal transformation by the rate given in Theorem 5 of Rubin-Delanchy et al. [14].

In this case, the indefinite orthogonal transformation W_* in the GRDPG result [14] is of the form $U^\top \hat{U}$. The eigenvalues of M are distinct since the signature for this GRDPG is $(1, 1)$, and $U^\top \hat{U}$ is block diagonal, resulting in $W_* \xrightarrow{P} I$. Therefore, the adjacency spectral embedding of $\hat{M}^{(kl)}$ is a direct estimation of the specific latent positions outlined for $M^{(kl)}$, up to sign flip.

4   Simulated Examples

For each simulation, the popularity vectors $\{\lambda^{(kl)}\}_K$ are drawn from a joint distribution, the edge probability matrix P is constructed using the popularity vectors, and finally an unweighted and undirected adjacency matrix A is drawn from P. Algorithm 2 is then used for community detection, and this method is compared against sparse subspace clustering [17] [13] and modularity maximization [16] [5]. True community labels are used with Algorithm 4

to estimate the popularity vectors, and this method is then compared against an MLE-based estimator described in Noroozi et al. [13] and Sengupta and Chen [16].

Sparse subspace clustering is described as follows. First, an embedding of the affinity matrix A is required, and for this, we use spectral decomposition using the first $K(K+1)/2$ and last $K(K-1)/2$ eigenvectors. Then a sparse linear regression model is fit to each row of the embedding data matrix using the remaining rows as predictors, the rows of which are stored in matrix C. Finally, an affinity matrix $B = |C| + |C|^\top$ is constructed, where $|\cdot|$ is applied entry-wise. If the data in the embedding lie perfectly in K subspaces, then $B_{ij} = 0$ for i, j not in the same subspace. If the embedding of P is used, then this property holds, but it is true in general for the embedding of A, in which case a final clustering step is required. For these simulations, spectral clustering with the normalized Laplacian and Gaussian mixture models is used for this final step.

Modularity maximization is NP-hard, so Sengupta and Chen [16] used the Extreme Points (EP) algorithm [10], which is $O(n^{K-1})$. For these simulations, the EP algorithm was used for $K = 2$, and for $K > 2$, the Louvain algorithm [4] was used instead.

4.1   Balanced communities

In each simulation, community labels $z_1, ..., z_n$ were drawn from a multinomial distribution with mixture parameters $\{\alpha_1, ..., \alpha_K\}$, then $\{\lambda^{(kl)}\}_K$ according to the drawn community labels, P was constructed using the drawn $\{\lambda^{(kl)}\}_K$, and A was drawn from P by $A_{ij} \overset{indep}{\sim} Bernoulli(P_{ij})$. Each simulation has a unique edge probability matrix P.

For these examples, we set the following parameters:

- Number of vertices $n = 128, 256, 512, 1024, 2048, 4096$
- Number of underlying communities $K = 2, 3, 4$
- Mixture parameters $\alpha_k = 1/K$ for $k = 1, ..., K$, (i.e., each community label has an equal probability of being drawn)
- Community labels $z_k \overset{\text{iid}}{\sim} Multinomial(\alpha_1, ..., \alpha_K)$
- Within-group popularities $\lambda^{(kk)} \overset{\text{iid}}{\sim} Beta(2, 1)$
- Between-group popularities $\lambda^{(kl)} \overset{\text{iid}}{\sim} Beta(1, 2)$ for $k \neq l$

50 simulations were performed for each (n, K) pair.

Fig 1 show that for large n, Algorithm 2 results in a misclustering rate of 0. Sparse subspace clustering produces similar results for $K > 2$.
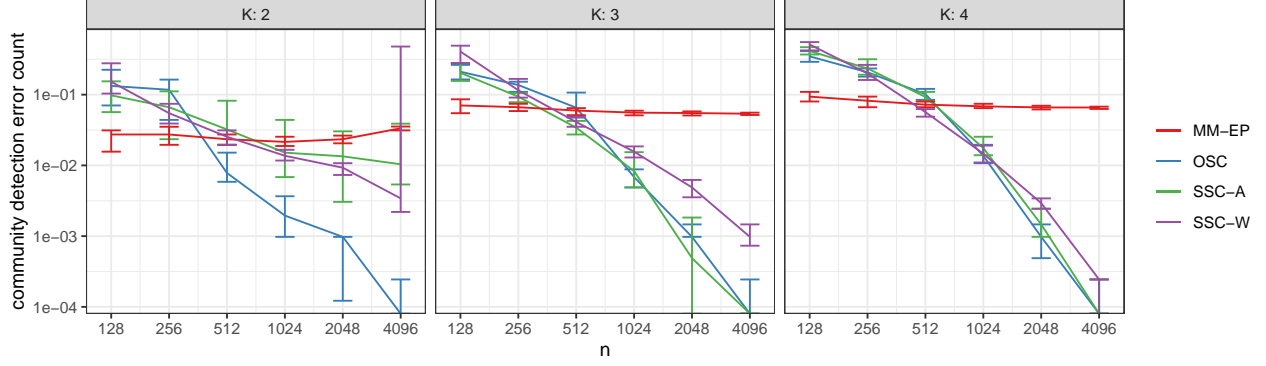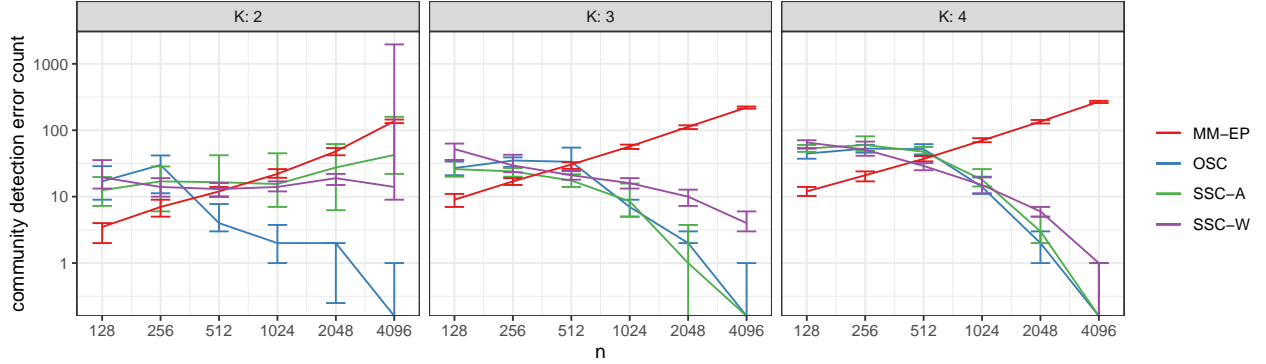
Figure 1: IQR of clustering error using Algorithm 2 (blue) compared against subspace clustering on the adjacency spectral embedding (green), the extreme points algorithm (red), and subspace clustering on the adjacency matrix, for sample sizes from 128 to 4096 and number of underlying communities from 2 to 4. Simulations were repeated 50 times for each sample size.

Theorem 4 implies that algorithm 2 will result in not just in the error rate converging to 0 but the error *count* as well (Fig. 2). We explore this in Fig 2.

Figure 2: IQR of counts of misclustered vertices using Algorithm 2 (blue) compared against subspace clustering on the adjacency spectral embedding (green), the extreme points algorithm (red), and subspace clustering on the adjacency matrix, for sample sizes from 128 to 4096. Simulations were repeated 50 times for each sample size.

Given ground truth community labels, Algorithm 5 and the MLE-based plug-in estimators [16] [13] perform similarly, with root mean square error decaying at rate approximately $n^{-1/2}$.
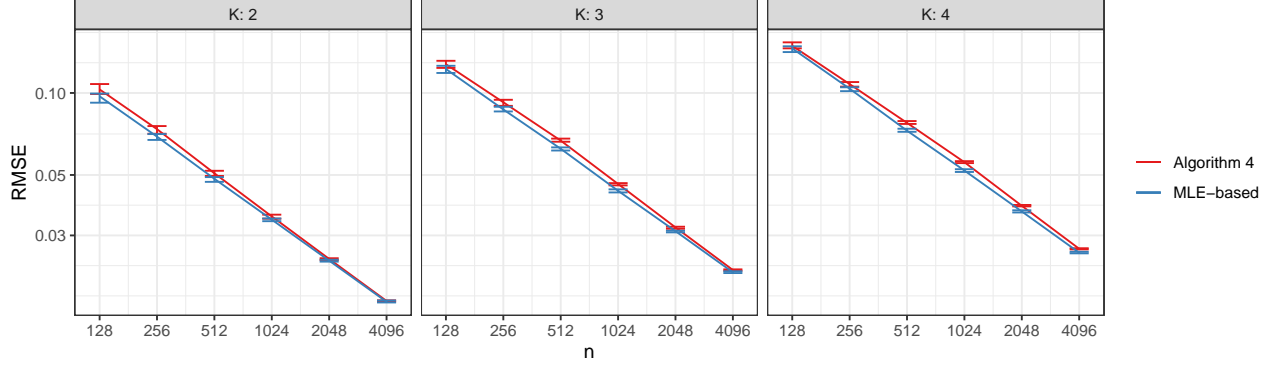
Figure 3: Median and IQR RMSE from Algorithm 4 (red) compared against an MLE-based method (blue) using sample sizes from 128 to 4096 and number of clusters from 2 to 4. Simulations were repeated 50 times for each sample size.

4.2 Imbalanced communities

Simulations performed in this section are similar to those in the previous section with the exception of the mixture parameters $\{\alpha_1, ..., \alpha_K\}$ used to draw community labels from the multinomial distribution. For these examples, we set the following parameters:

- Number of vertices $n = 128, 256, 512, 1024, 2048, 4096$
- Number of underlying communities $K = 2, 3, 4$
- Mixture parameters $\alpha_k = \frac{k^{-1}}{\sum_{l=1}^{K} l^{-1}}$ for $k = 1, ..., K$
- Community labels $z_k \overset{\text{iid}}{\sim} Multinomial(\alpha_1, ..., \alpha_K)$
- Within-group popularities $\lambda^{(kk)} \overset{\text{iid}}{\sim} Beta(2, 1)$
- Between-group popularities $\lambda^{(kl)} \overset{\text{iid}}{\sim} Beta(1, 2)$ for $k \neq l$

50 simulations were performed for each (n, K) pair.

Fig 4 and 5 show similar results as in the balanced communities case, with both Algorithm 2 and sparse subspace clustering resulting in no misclustered vertices for a sufficiently large sample size. However, Fig 6 suggests that while Algorithm 5 retains $\sqrt{n}$ efficiency, the MLE-based plug-in estimator fails to do so.
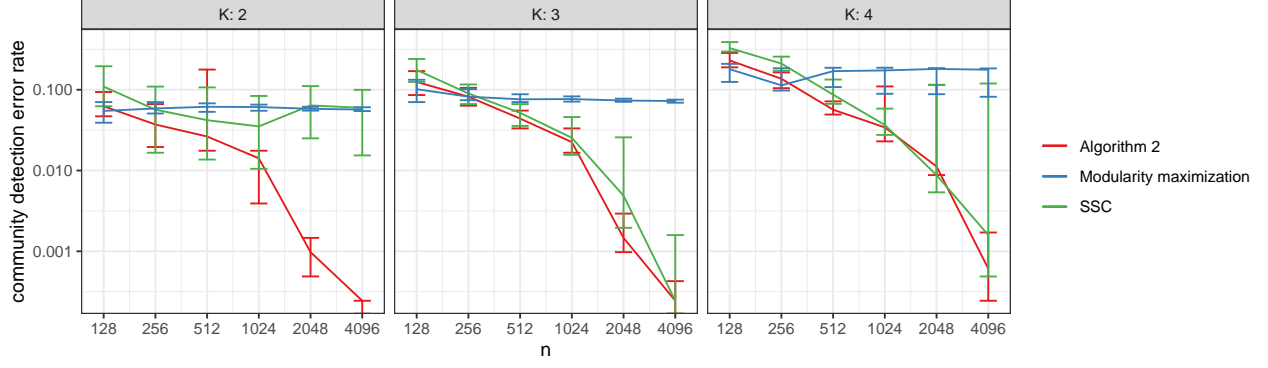
Figure 4: IQR of clustering error using Algorithm 2 (red) compared against modularity maximization (blue) and subspace clustering (green) for sample sizes from 128 to 4096 and number of clusters from 2 to 4. Simulations were repeated 50 times for each sample size.
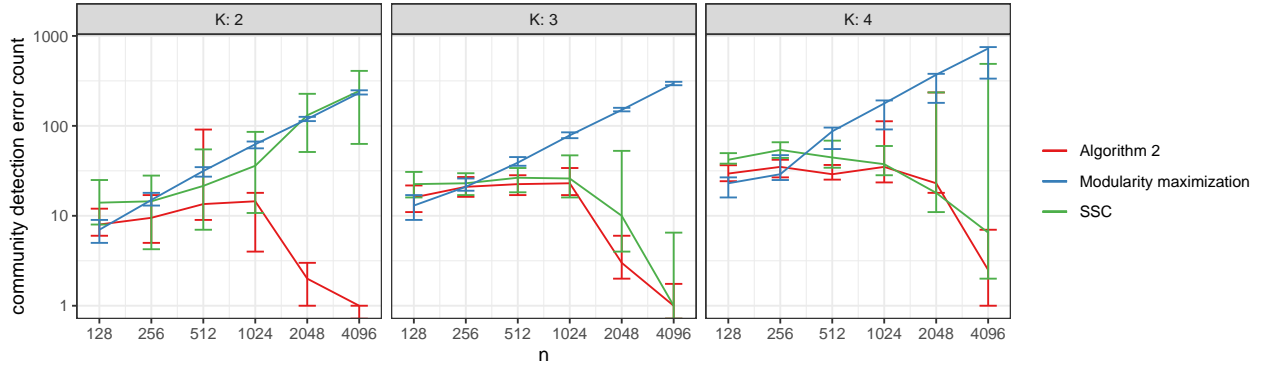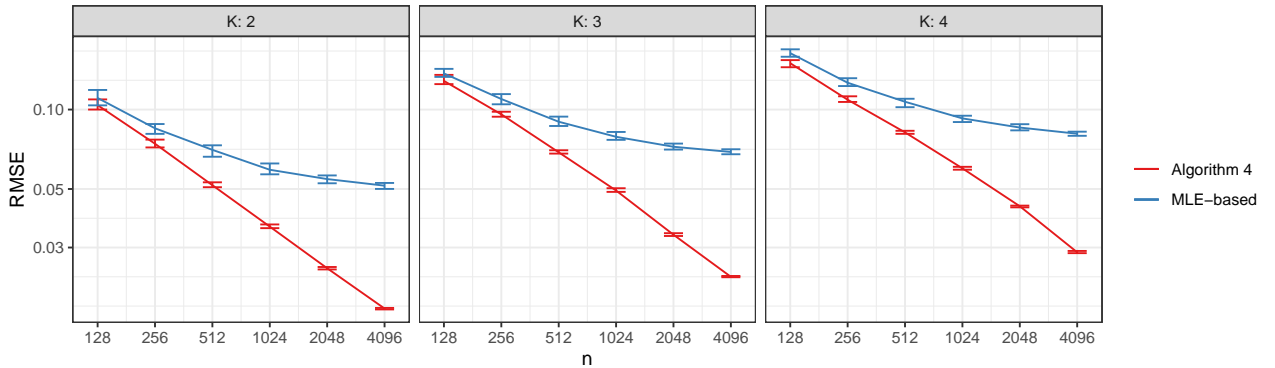

Figure 5: IQR of counts of misclustered vertices using Algorithm 2 (red) compared against subspace clustering (blue) for sample sizes from 128 to 4096. Simulations were repeated 50 times for each sample size.

Figure 6: Median and IQR RMSE from Algorithm 4 (red) compared against an MLE-based method (blue) using sample sizes from 128 to 4096 and number of clusters from 2 to 4. Simulations were repeated 50 times for each sample size.

4.3 Additional experiments

Using the same set of parameters for generating P and A as in the balanced communities examples for $K = 2$, we generated one instance of A for each n and constructed B according to algorithm 4 to verify that as $n \to \infty$, $(\hat{v}_i)^\top \hat{v}_j \xrightarrow{P} 0$ for i, j in different clusters. Furthermore, the distribution of these inner products should be approximately normal.
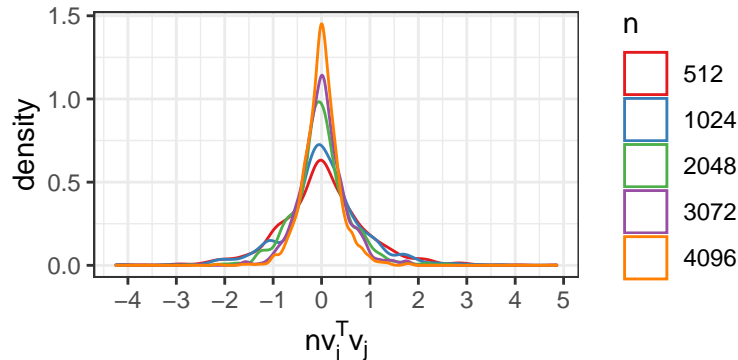

Figure 7: Between-cluster inner products of the eigenvectors of A for varying sample sizes.

5 Real data examples

In the first real data example, we applied Algorithm 2 to the Leeds Butterfly dataset [18] consisting of visual similarity measurements among 832 butterflies across 10 species. The graph was modified to match the example from Noroozi et al. [13]: Only the 4 most frequent species were considered, and the similarities were discretized to $\{0, 1\}$ via thresholding. Fig. 8 shows a sorted adjacency matrix sorted by the resultant clustering.

Comparing against the ground truth species labels, Algorithm 2 achieves an accuracy of 63% and an adjusted Rand index of 73%. In comparison, Noroozi et al. [13] achieved an adjusted Rand index of 73% using sparse subspace clustering on the same dataset.
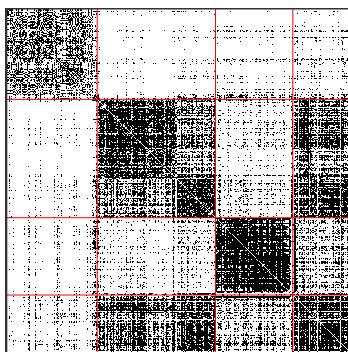

Figure 8: Adjacency matrix of the Leeds Butterfly dataset after sorting by the clustering outputted by Algorithm 2.

In the second example, we applied Algorithm 2 to the British MPs Twitter network [7],

the Political Blogs network [1], and the DBLP network [6] [8]. For this data analysis, we subsetted the data as described by Sengupta and Chen [16] for their analysis of the same networks. Our methods underperformed compared to modularity maximization, although performance is comparable. In addition, Algorithm 2's runtime is much lower than that of modularity maximization.

Table 1: Community detection error rates for modularity maximization, sparse subspace clustering, and Alg. 2.

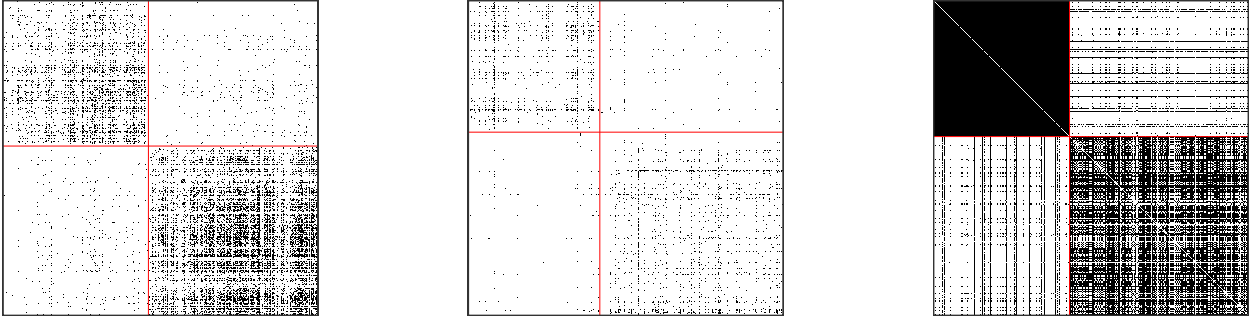| Network	Vertices	Error (Mod. Max.)	Error (SSC)	Error (Alg. 2)
British MPs	329	0.003	0.018	0.009
Political blogs	1222	0.050	0.196	0.062
DBLP	2203	0.028	0.087	0.059

Figure 9: Adjacency matrices of (from left to right) the British MPs, Political Blogs, and DBLP networks after sorting by the clustering outputted by Algorithm 2.

In the third example, we consider the Karantaka villages data studied by Banerjee et al. [3]. For this example, we chose the `visitgo` networks from villages 12, 31, and 46 at the household level. The label of interest is the religious affiliation. The networks were truncated to religions "1" and "2", and vertices of degree 0 were removed.
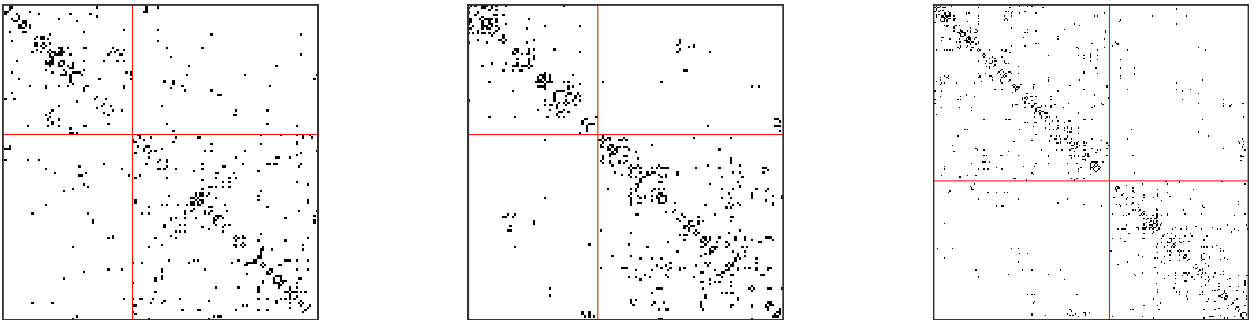

Figure 10: Adjacency matrix of the Karnataka villages data, arranged by the clustering produced by Algorithm 2 (left). The villages studied here are, from left to right, 12, 31, and 46.

Table 2: Community detection error rates for identifying household religion.

Method	Error (Village 12)	Error (Village 31)	Error (Village 46)
Alg. 2	0.227	0.110	0.078
SSC	0.291	0.169	0.307
Mod. Max.	0.270	0.125	0.052

6 Discussion

References

[1] Lada A. Adamic and Natalie Glance. The political blogosphere and the 2004 u.s. election: Divided they blog. In *Proceedings of the 3rd International Workshop on Link Discovery*, LinkKDD '05, page 36–43, New York, NY, USA, 2005. Association for Computing Machinery. ISBN 1595932151. doi: 10.1145/1134271.1134277. URL https://doi.org/10.1145/1134271.1134277.

[2] Edo M Airoldi, David M. Blei, Stephen E. Fienberg, and Eric P. Xing. Mixed membership stochastic blockmodels. In D. Koller, D. Schuurmans, Y. Bengio, and L. Bottou, editors, *Advances in Neural Information Processing Systems 21*, pages 33–40. Curran Associates, Inc., 2009. URL http://papers.nips.cc/paper/3578-mixed-membership-stochastic-blockmodels.pdf.

[3] Abhijit Banerjee, Arun G. Chandrasekhar, Esther Duflo, and Matthew O. Jackson. The Diffusion of Microfinance, 2013. URL https://doi.org/10.7910/DVN/U3BIHX.

[4] Vincent D Blondel, Jean-Loup Guillaume, Renaud Lambiotte, and Etienne Lefebvre. Fast unfolding of communities in large networks. *Journal of Statistical Mechanics: Theory and Experiment*, 2008(10):P10008, Oct 2008. ISSN 1742-5468. doi: 10.1088/1742-5468/2008/10/p10008. URL http://dx.doi.org/10.1088/1742-5468/2008/10/P10008.

[5] Gabor Csardi and Tamas Nepusz. The igraph software package for complex network research. *InterJournal*, Complex Systems:1695, 2006. URL https://igraph.org.

[6] Jing Gao, Feng Liang, Wei Fan, Yizhou Sun, and Jiawei Han. Graph-based consensus maximization among multiple supervised and unsupervised models. In Y. Bengio, D. Schuurmans, J. D. Lafferty, C. K. I. Williams, and A. Culotta, editors, *Advances in Neural Information Processing Systems 22*, pages 585–593. Curran Associates, Inc., 2009. URL http://papers.nips.cc/paper/3855-graph-based-consensus-maximization-among-multiple-supervised-and-unsupervised-models.pdf.

[7] Derek Greene and Pádraig Cunningham. Producing a unified graph representation from multiple social network views. *CoRR*, abs/1301.5809, 2013. URL http://arxiv.org/abs/1301.5809.

[8] Ming Ji, Yizhou Sun, Marina Danilevsky, Jiawei Han, and Jing Gao. Graph regularized transductive classification on heterogeneous information networks. In José Luis Balcázar, Francesco Bonchi, Aristides Gionis, and Michèle Sebag, editors, *Machine Learning and Knowledge Discovery in Databases*, pages 570–586, Berlin, Heidelberg, 2010. Springer Berlin Heidelberg. ISBN 978-3-642-15880-3.

[9] Brian Karrer and M. E. J. Newman. Stochastic blockmodels and community structure in networks. *Physical Review E*, 83(1), Jan 2011. ISSN 1550-2376. doi: 10.1103/physre ve.83.016107. URL http://dx.doi.org/10.1103/PhysRevE.83.016107.

[10] Can M. Le, Elizaveta Levina, and Roman Vershynin. Optimization via low-rank approximation for community detection in networks. *Ann. Statist.*, 44(1):373–400, 02 2016. doi: 10.1214/15-AOS1360. URL https://doi.org/10.1214/15-AOS1360.

[11] François Lorrain and Harrison C. White. Structural equivalence of individuals in social networks. *The Journal of Mathematical Sociology*, 1(1):49–80, 1971. doi: 10.1080/0022 250X.1971.9989788. URL https://doi.org/10.1080/0022250X.1971.9989788.

[12] Vince Lyzinski, Daniel L. Sussman, Minh Tang, Avanti Athreya, and Carey E. Priebe. Perfect clustering for stochastic blockmodel graphs via adjacency spectral embedding. *Electron. J. Statist.*, 8(2):2905–2922, 2014. doi: 10.1214/14-EJS978. URL https://doi.org/10.1214/14-EJS978.

[13] Majid Noroozi, Ramchandra Rimal, and Marianna Pensky. Estimation and Clustering in Popularity Adjusted Stochastic Block Model. *arXiv e-prints*, art. arXiv:1902.00431, February 2019.

[14] Patrick Rubin-Delanchy, Joshua Cape, Minh Tang, and Carey E. Priebe. A statistical interpretation of spectral embedding: the generalised random dot product graph, 2017.

[15] Patrick Rubin-Delanchy, Carey E. Priebe, and Minh Tang. Consistency of adjacency spectral embedding for the mixed membership stochastic blockmodel, 2017.

[16] Srijan Sengupta and Yuguo Chen. A block model for node popularity in networks with community structure. *Journal of the Royal Statistical Society. Series B: Statistical Methodology*, 80(2):365–386, March 2018. ISSN 1369-7412. doi: 10.1111/rssb.12245.

[17] Mahdi Soltanolkotabi, Ehsan Elhamifar, and Emmanuel J. Candès. Robust subspace clustering. *Ann. Statist.*, 42(2):669–699, 04 2014. doi: 10.1214/13-AOS1199. URL https://doi.org/10.1214/13-AOS1199.

[18] Bo Wang, Armin Pourshafeie, Marinka Zitnik, Junjie Zhu, Carlos D. Bustamante, Serafim Batzoglou, and Jure Leskovec. Network enhancement as a general method to denoise weighted biological networks. *Nature Communications*, 9(1), Aug 2018. ISSN 2041-1723. doi: 10.1038/s41467-018-05469-x. URL http://dx.doi.org/10.1038/s41467-018-05469-x.

[19] Stephen J. Young and Edward R. Scheinerman. Random dot product graph models for social networks. In Anthony Bonato and Fan R. K. Chung, editors, *Algorithms and Models for the Web-Graph*, pages 138–149, Berlin, Heidelberg, 2007. Springer Berlin Heidelberg. ISBN 978-3-540-77004-6.